The Journal of Experimental Biology 213, 1115-1125

doi:10.1242/jeb.035618

Slippery surfaces of pitcher plants: *Nepenthes* wax crystals minimize insect attachment *via* microscopic surface roughness

I. Scholz[1], M. Bückins[2], L. Dolge[1], T. Erlinghagen[1], A. Weth[1], F. Hischen[1], J. Mayer[2], S. Hoffmann[3], M. Riederer[4], M. Riedel[4] and W. Baumgartner[1,*]

[1]RWTH-Aachen University, Department of Cellular Neurobionics, Kopernikusstrasse 16, 52056 Aachen, Germany, [2]RWTH-Aachen University, Central Facility for Electron Microscopy, Ahornstrasse 55, 52056 Aachen, Germany, [3]RWTH-Aachen University, Department of Ferrous Metallurgy, Intzestrasse 1, 52072 Aachen, Germany and [4]Universität Würzburg, Julius-von-Sachs-Institut für Biowissenschaften, Lehrstuhl für Botanik II, Julius-von-Sachs-Platz 3, 97082 Würzburg, Germany

*Author for correspondence (werner@bio2.rwth-aachen.de)

Accepted 6 December 2009

SUMMARY

Pitcher plants of the genus *Nepenthes* efficiently trap and retain insect prey in highly specialized leaves. Besides a slippery peristome which inhibits adhesion of insects they employ epicuticular wax crystals on the inner walls of the conductive zone of the pitchers to hamper insect attachment by adhesive devices. It has been proposed that the detachment of individual crystals and the resulting contamination of adhesive organs is responsible for capturing insects. However, our results provide evidence in favour of a different mechanism, mainly based on the stability and the roughness of the waxy surface. First, we were unable to detect a large quantity of crystal fragments on the pads of insects detached from mature pitcher surfaces of *Nepenthes alata*. Second, investigation of the pitcher surface by focused ion beam treatment showed that the wax crystals form a compact 3D structure. Third, atomic force microscopy of the platelet-shaped crystals revealed that the crystals are mechanically stable, rendering crystal detachment by insect pads unlikely. Fourth, the surface profile parameters of the wax layer showed striking similarities to those of polishing paper with low grain size. By measuring friction forces of insects on this artificial surface we demonstrate that microscopic roughness alone is sufficient to minimize insect attachment. A theoretical model shows that surface roughness within a certain length scale will prevent adhesion by being too rough for adhesive pads but not rough enough for claws.

Supplementary material available online at http://jeb.biologists.org/cgi/content/full/213/7/1115/DC1

Key words: *Nepenthes*, slippery surface, tribology, plant–insect interaction, carnivorous plants, attachment, focused ion beam, atomic force microscopy.

INTRODUCTION

Plants of the carnivorous genus *Nepenthes* (Nepenthaceae) efficiently attract, trap, retain and finally digest animal prey in highly modified leaves (Juniper et al., 1989). Within these pitcher-shaped leaves, different functional zones can be distinguished by their morphological and physicochemical surface characteristics, all of which contribute to the carnivorous syndrome (Knoll, 1914; Juniper et al., 1989; Gaume et al., 2002; Gaume et al., 2004; Bohn and Federle, 2004). The opening of these pitchers is lined by the peristome, which plays an important role in prey attraction by visual and olfactory cues and by nectar secreted at its inner margin (Moran, 1996; Owen and Lennon, 1999; Lloyd, 1942). It is also important for the trapping of insects, which slide on its fully wettable anisotropic surface (Bohn and Federle, 2004; Bauer et al., 2008). The surface of the conductive zone immediately below the peristome has also been recognized as essential for trapping and retaining insect prey, but in this case due to its special downward-directed lunate cells and its coverage with a thick layer of epicuticular wax crystals (McFarlane, 1893; Knoll, 1914). In spite of these very different mechanisms, both surfaces are extremely slippery for insects and cause the prey to fall into the lower part of the pitcher. In this part, specialized glands secrete a digestive solution in which the insects get trapped (Gaume and Forterre, 2007) and which finally absorbs the insect-derived nutrients (An et al., 2002a; An et al., 2002b; Schulze et al., 1997; Owen and Lennon, 1999; Owen et al., 1999).

Surface attachment of insects is principally enabled by the interlocking of hard claws and/or adhesion of flexible attachment devices to a wide variety of substrates (Beutel and Gorb, 2001). At the cellular level of both *Nepenthes* pitcher surfaces, trapping efficiency is enhanced by the anisotropic arrangement of smooth overlapping epidermal cells (Bohn and Federle, 2004; Gaume et al., 2004). This arrangement only allows the interlocking of insect tarsal claws during inward locomotion of the prey. Escape from the pitcher by using adhesive pads is also hampered by the physicochemical properties of the cuticular surfaces of the different pitcher zones. The peristome was shown to be completely wettable by nectar or rain water, leading to coverage with homogeneous liquid films that impede close contact between the plant and tarsal pad surfaces (Bohn and Federle, 2004). For the conductive zone, several mechanisms for its slipperiness have been discussed. As early as 1914, Knoll noted that the epicuticular wax crystals on the surface are easily detachable under the weight load of an insect foot, leading to contamination and hence inactivation of the adhesive device (Knoll, 1914). This interpretation was supported by the observation that crystal platelets are fastened to lower epicuticular layers by thin fragile ‘stalks’ (Juniper and Burras, 1962; Gorb et al., 2005). Experiments

on flies (*Calliphora vomitoria*) walking on the waxy surface of *Nepenthes ventrata* supported this theory: after 10 min of walking little contamination of the adhesive setae was found but after 2 h the tarsus was completely covered (Gaume et al., 2004). However, investigations that used mechanical sampling strategies to prepare the crystals selectively (Riedel et al., 2003; Riedel et al., 2007) showed that the outermost crystals visible in the SEM do not consist of independent platelets but form a continuous 3D network of interconnected structures that keeps its structural integrity even after mechanical removal from the plant surface (Riedel et al., 2003; Riedel et al., 2007). These observations suggest that the extreme slipperiness of the waxy pitcher walls for insects cannot simply be explained by the fracture and detachment of wax crystals. In this study we investigated the mechanism of slipperiness by combining scanning electron microscopy (SEM), focused ion beam (FIB) treatment, atomic force microscopy (AFM) and attachment tests on live insects. We addressed the following questions. (1) How is the wax structure arranged beneath the outermost crystal parts? (2) What force values are necessary to break off the outermost crystal parts? (3) Do insect adhesive pads get contaminated by detached wax crystals? (4) Is the breaking of wax crystals necessary to capture prey?

MATERIALS AND METHODS

Plant material

Specimens of *Nepenthes alata* Blanco (Nepenthaceae) were taken from a continuous greenhouse culture in the Botanical Garden of the University of Würzburg. Pitchers open for approximately 7 days were freshly harvested for preparations. Rectangular leaf sections of 10–15 mm side length were cut from the conductive zone and either air dried for FIB imaging or freshly used without further preparation for AFM measurements (see below).

Study animals

Female stick insects (*Carausius morosus* Sinety, Phasmatidae) were taken from a laboratory colony. Juvenile specimens (larval state L1–L3; length 20–25 mm; mass 19–88 mg) were used for centrifugation experiments. For slip-off experiments juveniles of larval state L3–L5 (length 40–65 mm, mass 144–539 mg) were used. Additionally, living adult black garden ants (*Lasius niger* L., Formicidae) were captured near the research department in Aachen (Germany).

Ants are the native prey of *Nepenthes*, thus these insects were of greatest interest; however, experiments were also performed with stick insects, because these have similar adhesive pads which are, in contrast to those of ants, very well characterized with respect to mechanical properties. This allows theoretical modelling (see below).

Artificial surfaces

For friction force measurements, comparison to the glaucous *Nepenthes* surface, and calculation of a model for the interaction of insect tarsi with structured surfaces we used artificial surfaces with different surface parameters. As a flat and relatively non-structured surface we used polycarbonate. Surfaces with different profile parameters were represented by different types of polishing paper. The grain sizes of the so-called microgrits abrasive are defined by the sedimentation time of the particles. The particles are made of silicon carbide. Further information on particle size and size distribution is given by the FEPA-standards 42-2:2006, 43-2: 2006 and ISO 6344 and 8486 (Federation of European Producers of Abrasives, France).

The polishing paper (Mirka, Karlsruhe, Germany) and its mean grain sizes (in brakes) used in our experiments were: P320 (46.2±1.5 μm), P600 (25.8±1 μm), P2000 (10.3±0.8 μm) and P4000 (3.0±0.5 μm).

SEM imaging

For SEM imaging, air-dried pitcher material from the conductive zone was sputter-coated with gold for 8 min with a sputter current of 10 mA, resulting in a gold layer of less than 2 nm. Observations were made using a Stereoscan S604 SEM (Cambridge Scientific Instruments Ltd, Cambridge, UK). Images were digitally recorded using an attached i-scan digitizer (ISS Group Services Ltd, Manchester, UK) with an image acquisition time of 50 s.

FIB treatment

For determining 3D structure, FIB cutting was performed using a Strata FIB 205 (FEI, Hillsborough, OR, USA) single beam workstation. A focused beam of Ga ions from a liquid metal source was projected onto the gold-coated specimen. The gold coating was approximately 100 nm thick in order to prevent the surface from immediate damaging by the Ga ions. An acceleration voltage of 30 kV was used and the beam current was adjusted to 30 pA for imaging of the surface, which was observed without further treatment. Typically for cutting, a beam current of 300 pA was used and the cutting edge was finally polished using a beam current of 50 pA. However, the beam current for cutting was varied for control purposes from 10 to 1000 pA in order to exclude artefacts due to local heating.

AFM measurements

AFM measurements were performed using a commercially available AFM (Explorer, Veeco Instruments, Woodbury, NY, USA) equipped with a 100 μm scanner. For imaging the scale topography the AFM was equipped with high reflection coated triangular silicon nitride cantilevers (Type MLCT, Veeco Instruments) with a nominal spring constant of 0.5 $N\,m^{-1}$, a four-sided pyramidal tip with a tip angle of 35 deg. (centreline-to-face) and a tip radius of 20 nm. Scanning was performed in contact mode to obtain information about the stability of the glaucous surface on *N. alata*. The scanning force was adjusted from 20 nN to 250 nN and images were obtained at various scanning velocities ranging from 1 $\mu m\,s^{-1}$ to 50 $\mu m\,s^{-1}$. Scans were performed at room temperature in an aqueous solution containing 5 g NaCl, 0.15 g KCl, 0.25 g CaCl, 0.15 g $NaHCO_3$ in 1 l pure water, pH 7.4. The freshly cut plant material (approximately 15 mm×15 mm) was glued using hot glue onto the bottom of a Petri dish. The glue was only applied to the corners of the square in order to avoid structural changes of the wax. The Petri dish was immediately filled with the aqueous solution and degassed in an evacuated desiccator. Immersion was found to be vital in order to prevent artefacts due to shrinkage of the plant material. Furthermore, fresh material had to be used as dried plant material sometimes exhibited reduced stability of the wax crystals (see below).

Slip-off experiments

Three kinds of experiments were carried out to find out whether loose wax crystals from the conductive zone of *N. alata* would adhere to tarsi of insects and whether the intact wax layer of that region stays stable under the mechanical load of a slipping insect.

In the first of the experiments, wax from the conductive zone was separated from two pitchers and applied to a glass plate using a stiff paint brush. *Carausius morosus* and *L. niger* individuals were

put onto this glass plate to run on the loose pieces of wax for a few seconds.

In the second of the experiments, six pitchers open for about 12 h per day for up to 16 days were taken from a pool of *N. alata* grown under greenhouse conditions. The digestive zone and the lid were cut and the pitchers clamped in the horizontal direction approximately 10 cm above a beaker, filled with a gentle flow of CO_2. Specimens of *L. niger* and *C. morosus* were put onto the waxy pitcher surface, directly underneath the peristome. The pitchers were then rotated to the vertical direction to induce slip-off into the beaker. On each pitcher surface this was carried out with three *L. niger* and one *C. morosus* individual. Afterwards, the insects from both the first and second experiments were anaesthetized with CO_2 and decapitated. The legs were cut off, air dried in a Petri dish on silica gel at a temperature of 28°C for 24 h and gold coated for 5 min (10 mA sputter current, gold layer less than 2 nm). Observations were made using the Stereoscan S604 SEM. Possible contamination of the adhesive organs, especially the arolii and tarsi, as well as the tarsal hairs by wax crystals or other wax residuals was documented. Pieces of the pitcher surfaces which the ants had slipped off were removed, air dried and gold sputtered. The waxy surfaces were observed using the SEM, to obtain information about the crystals after the insects had slipped off.

In the third of the slip-off experiments the ability of ants to cling to a smooth glass surface was tested: first, directly after walking on loose wax crystals; and second, after walking on an intact *Nepenthes* wax surface. Two watch glasses were prepared: the first with loose wax brushed from dry pitcher surfaces and the second with pieces of an intact wax layer on the bottom. After the ants were put onto the watch glass it was covered with a cleaned glass tube. The movement of the ants was filmed using a standard digital photo camera to get information on the ants' ability to cling to the smooth glass after walking on wax crystals and the intact wax layer.

Surface profile parameters

Surface profile parameters of the polishing paper P4000 and the glaucous *Nepenthes* surface were obtained using a µsurf customized (NanoFocus, Oberhausen, Germany) Confocal-Multi-Pinhole microscope. Employing an ocular lens with ×100 magnification, the parameters R_a (roughness average), R_q (root mean square roughness), R_{Pc} (roughness peak count) and R_{Sm} (mean spacing of profile irregularities) were determined with regard to DIN EN ISO standards.

Friction measurement by centrifugation

To measure attachment forces of *C. morosus* and *L. niger*, we used a centrifuge technique in order to determine the maximal frictional force, similar to the method described by Federle and colleagues (Federle et al., 2000; Federle et al., 2004). Insects were placed on a turntable coated with either a flat polycarbonate plate or polishing paper (see above). A strobe light synchronized to the revolutions of the centrifuge through a photoelectric barrier was used for illumination so that a standing image of the insect on the rotating surface could be seen. The centrifuge was filmed from above (distance 0.9 m) with a standard 25 Hz CCD video camera (Panasonic F15).

Revolutions per minute of the centrifuge were recorded with the stroboscope and the radius at which the insect detached was measured by marks placed at 10 mm radial intervals on the surface under investigation. *Carausius morosus* and *L. niger* individuals were placed on the turntable and the rotation was slowly accelerated until detachment occurred. The centrifugal force at the time of detachment was taken as the friction force reached by the insect under investigation. As shown previously (Federle et al., 2004), other forces are small in comparison to the centrifugal force. Additionally, in the present study only relative changes and not the exact absolute values of the forces are important, yielding the described method sufficient and adequate. The adhesion forces were measured on polishing papers with grain sizes P320, P600, P2000 and P4000 and a flat polycarbonate surface for both species (*C. morosus* and *L. niger*; N=10).

RESULTS

Scanning electron microscopic investigation of *N. alata* pitchers (Fig. 1) revealed exactly the morphology previously described in the literature (Riedel et al., 2003; Riedel et al., 2007; Gaume et al.,

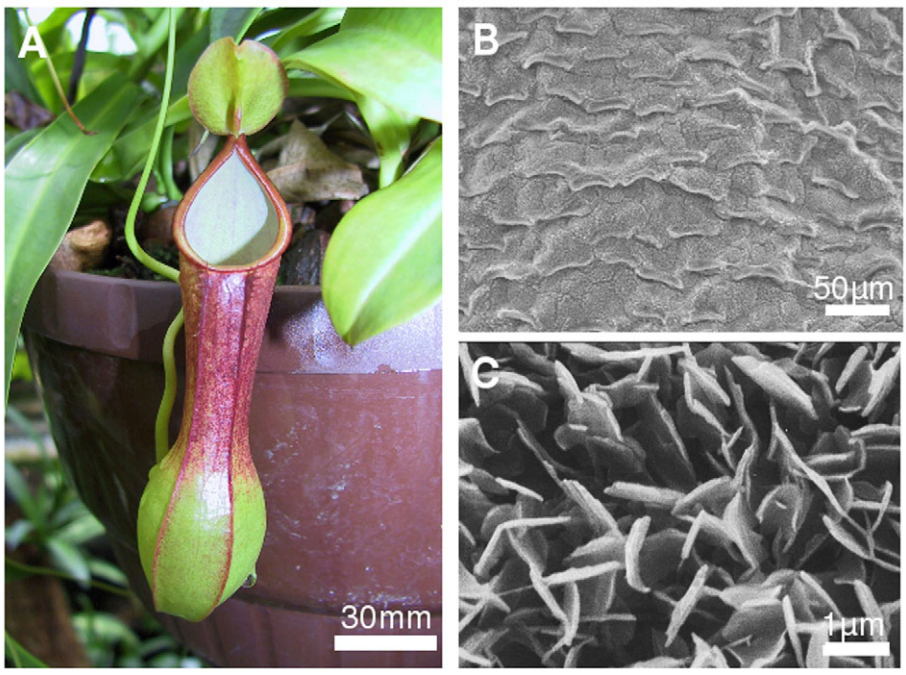

Fig. 1. Morphology of a pitcher of the carnivorous plant *Nepenthes alata*. (A) Macroscopic view. The opening of the pitcher is lined by the peristome with a fully wettable, anisotropic surface. The inner pitcher wall of the conductive zone is covered by a thick, glaucous and super-hydrophobic layer of epicuticular wax crystals. (B) Scanning electron microscope (SEM) image of the conductive zone from an air-dried pitcher. The epidermis is characterized by modified stomata that hamper interlocking of insect tarsal claws and by coverage of the cuticle with a continuous layer of epicuticular wax crystals. (C) The outermost parts of the epicuticular wax platelets stand upright exposing their narrow sides to the lumen of the pitcher and, thus, represent the top layer of a more complex crystalline structure that lies underneath and extends to the cuticle surface.

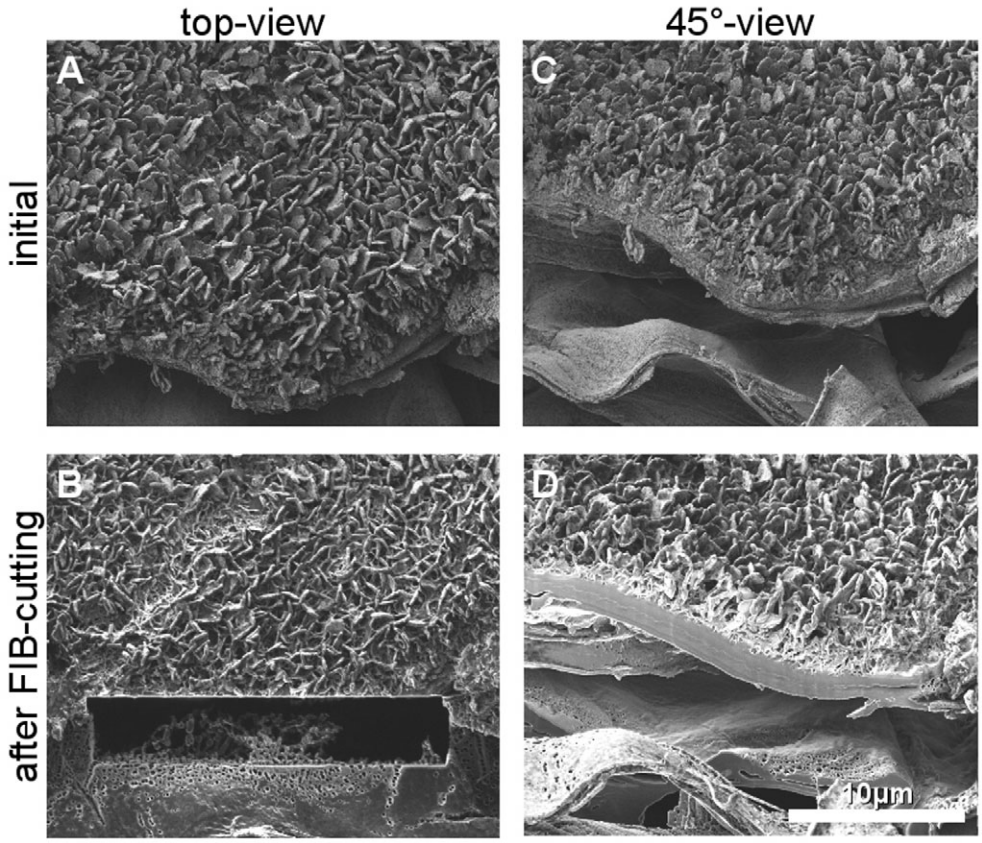

Fig. 2. Focused ion beam (FIB) cutting of plant material. A position at the scissor-cut edge of the plant material from the conductive zone was chosen where only a little damage to the cut edge was visible and which exhibits a convex form. This is shown in A and C in a top view (A) and a 45 deg. view (C) of the identical position. After cutting out a rectangular pattern and polishing (B), a sharply cut smooth surface becomes visible when observed at an angle of 45 deg. (D). Scale bar applies to A–D.

2004). Because of a dense wax bloom immediately below the rim of the pitcher, the inner wall surface of the conductive zone appears glaucous (Fig. 1A). In SEM this wax bloom was shown to cover all epidermal cells, including the lunate cells, as a continuous layer (Fig. 1B). Platelet-shaped wax crystals with entire margins protruded from the underlying structures, standing almost upright and therefore exposing their narrow sides to the lumen of the pitcher (Fig. 1C). Angles between the outermost crystal parts showed no preference, creating a random pattern of small air spaces in between (Riedel et al., 2003). In order to clarify the 3D structure of the epicuticular wax layer and thereby the organization of the wax crystals, FIB cutting was performed. This technique was found to be necessary because freeze fracture of the wax crystal zone yielded samples with damaged breaking edges. For FIB cutting, gold-coated samples of the conductive zone were used with an apparently intact wax layer in the proximity of the cutting edge (Fig. 2A,C). A rectangular area of about 20 µm×5 µm was cut from the sample (Fig. 2B,D) and the FIB-cut edge was finally ion-polished. Scanning electron micrographs of the FIB-cut edge at higher magnifications (Fig. 3) clearly showed the 3D structure of the epicuticular wax. Instead of a single layer of isomorphic platelet-shaped crystals, a sponge-like or trabecular structure became evident. This sponge-like layer showed a fairly constant thickness of about 3 µm and the mesh size of the sponge decreased towards the compact lower epicuticular wax layer. Apparently, the platelet-shaped crystals described so far are only the outermost walls of this porous structure. To rule out artefacts due to local heating by the FIB, the experiments were repeated with different ion currents. As the structures observed were approximately identical in all samples (not shown), we were able to conclude that no local heating took place which would have led to structural changes dependent on the ion current.

It appears unlikely that these trabecular cross-linked structures will be detached under the weight of insects leading to contamination and hence inactivation of the adhesive devices as suggested by Knoll and others (Knoll, 1914; Juniper and Burras, 1962; Gorb et al., 2005). However, in order to understand the mechanical properties and to find out whether detachment of crystal parts of the sponge-like wax layer alone can be responsible for the anti-adhesive properties of

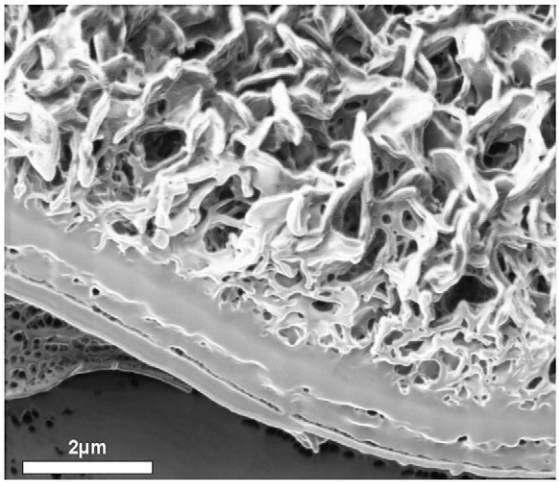

Fig. 3. High-resolution image of a polished surface observed at an angle of 45 deg. It is evident that the epicuticular wax consists of a spongy structure of approximately 3 µm thickness, protruding from more compact layers of about 2 µm that represent a cross-section of the periclinal cell wall and the superimposed cuticular membrane.

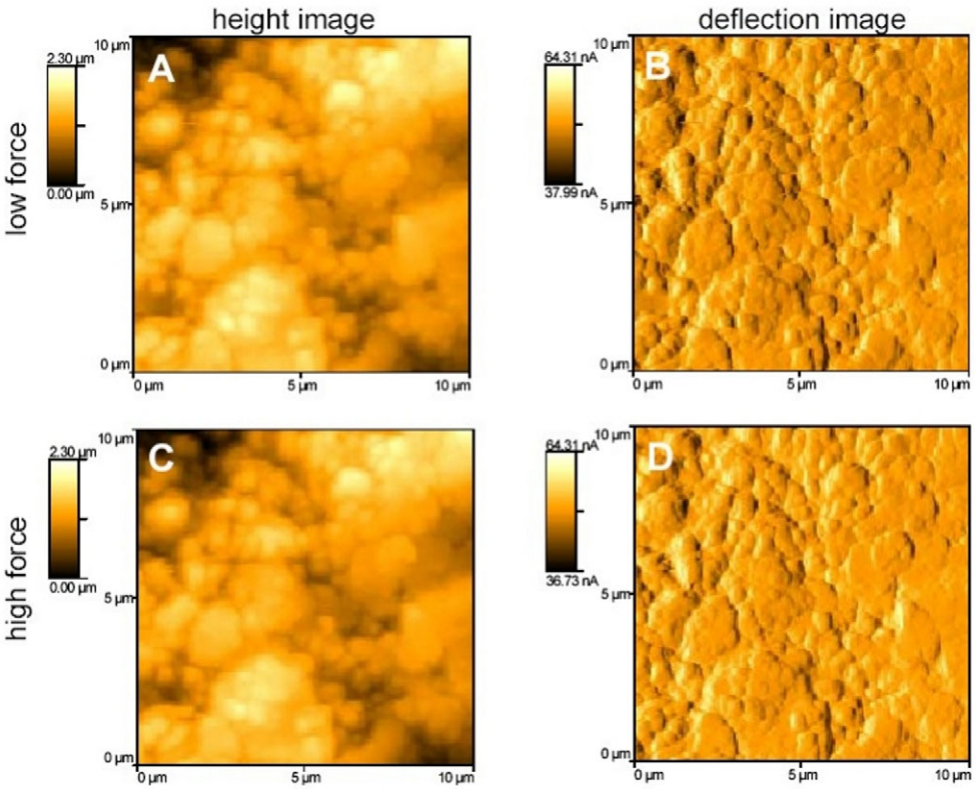

Fig. 4. Atomic force microscopy (AFM) images of the wax surface of the conducting zone of *Nepenthes* pitchers. The surface was scanned repeatedly at different forces, starting with low scanning forces of 20 nN (A,B) and ranging to high forces of 250 nN (C,D). As evident from height (A,C) and deflection images (B,D), no change in surface morphology can be observed. The AFM images resemble exactly the wax structures observed in the SEM images when taking the tip effects into account (see text).

the conductive zone, AFM was performed. This was done using freshly prepared 1 cm^2 samples from the conductive zone, immersed in a slightly hypotonic salt solution. Using fresh material was necessary because the wax layer on dry material was found to be mechanically unstable in comparison with fresh material (data not shown). Immersion was found to be necessary because otherwise substantial shrinkage of the tissue during the AFM investigation occurred, disturbing the imaging process. Degassing of the immersed plant material was also essential as the wax layer is highly hydrophobic yielding a thin air film on the surface which would disturb the AFM measurements. This film, however, can be almost entirely removed by short (5 min) degassing in an evacuated desiccator.

Typical AFM images, obtained in the contact mode, are shown in Fig. 4. Because of the AFM tip geometry the thin and steep walls of the sponge-like wax layer could not be resolved in greater detail. The tip yields a wall perpendicular to the scanning direction appearing under an angle identical to the tip angle α, which is 35 deg. centreline-to-face in our case. This is depicted in principle in Fig. 5. Taking this fact into account, the AFM images very much resemble the structures observed under the SEM, showing that an intact wax layer was indeed scanned. The images obtained were not altered when scanning force, direction and/or speed were changed. Scanning forces (i.e. forces perpendicular to the surface) up to about F_N=250 nN could not destroy the wax structures (Fig. 4). Higher forces were not tested because of technical limitations of the apparatus and cantilevers used.

Considering the geometry shown in Fig. 5, we obtained the total force (F_{tot}) acting between the tip and a steep wall (wax crystal) to be $F_{tot}=F_N/\sin(\alpha)$. This results in a bending force $F_H=F_N/\tan(\alpha)$ of approximately 400 nN acting locally on the wax crystal. Thus, a single crystal, i.e. a single wall of the sponge-like structure, can at least withstand forces which correspond to a mass of 40 µg attached at the outermost edge of a single crystal. As this represents the maximum bending momentum we can assume this arrangement to be the worst case. A single adhesive organ of a typical prey insect has a contact area of more than 10,000 μm^2. According to the SEM and FIB images, the density of individual walls (crystals) is about 1 per μm^2. Thus, the force acting locally on a single crystal caused e.g. by a large ant of 5 mg is of the order of 5 nN, corresponding to 0.5 µg of attached mass per crystal if only one small arolium of a heavy ant is in contact (worst case), which is two orders of magnitude lower than the force

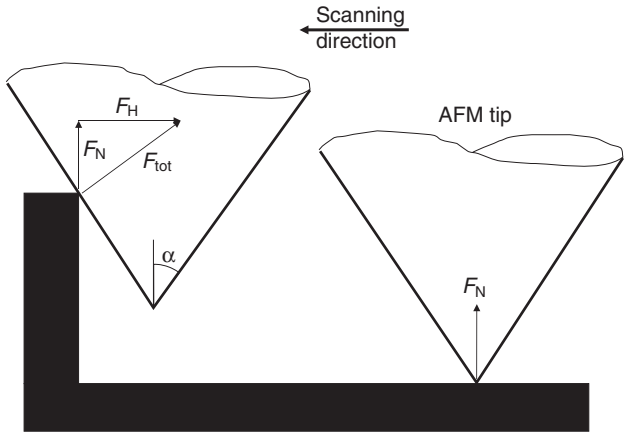

Fig. 5. Schematic drawing of the AFM tip scanning a wall-like structure. For scanning, the normal force F_N is used as the feedback parameter and kept constant. If the tip, having a finite tip angle of e.g. α=35 deg., hits a vertical wall, the total force F_{tot} will act normally on the pyramidal side of the tip. This force must be the vectoral addition of the normal force and a horizontal force F_H. The latter F_H results in a bending momentum and shear stress on the wall material (see text).

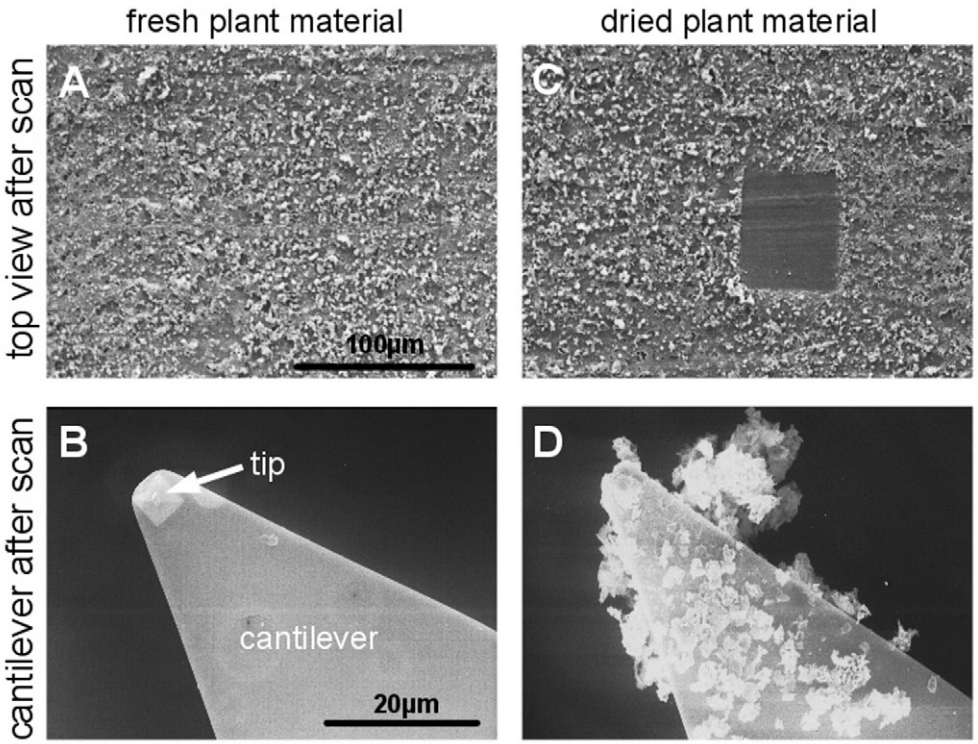

Fig. 6. Effects of AFM scans of detached wax crystals. Wax was removed by a drop of frozen water from the conductive zones of fresh *Nepenthes* pitchers. The surface looks identical to the native wax (A). After performing 50 µm×50 µm scans, rectangular areas of broken and/or removed wax crystals can be seen (C). New and clean AFM tips (B) are highly contaminated with wax crystals after scanning (D).

a single crystal can withstand in the experiment. Thus, even if only 1% of the area of the arolium is in contact, the crystals would still withstand the force acting upon them. For control experiments we repeated the AFM measurements on detached wax layers (removed by drops of frozen water) (Riedel et al., 2003) having an identical geometry but being less stable as only the outermost part of the wax is removed. As clearly demonstrated in Fig. 6, the AFM tip can break and/or remove these wax crystals. Thus, if considerable breaking of wax crystals took place on fresh, intact pitchers, the AFM technique in combination with the accompanying SEM investigation would detect this. However, we never found any evidence of breaking due to AFM scanning on intact pitchers as we always got stable AFM images and non-contaminated tips after scanning, and we never found areas of broken wax crystals.

In addition to the atomic force microscopy, slip-off experiments on intact pitchers as well as detached wax layers were performed. The results of the first of these experiments on detached wax layers clearly show that loose pieces of wax from the pitcher plants adhere to the arolia, hairs and claws of the tarsi of both insect species, *C. morosus* and *L. niger*. Fig. 7D,E clearly shows huge amounts of wax,

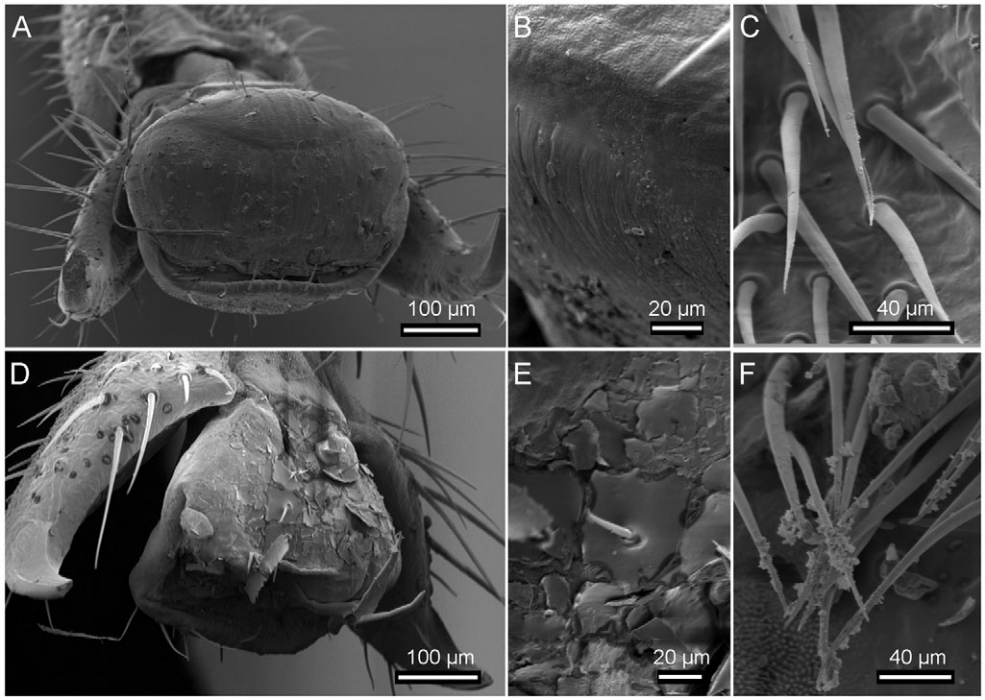

Fig. 7. Tarsi of the stick insect *Carausius morosus* after slipping off the waxy surface of *N. alata* pitchers (A–C) and after walking on loose pieces of wax (D–F); SEM images. Only a slight residue of wax crystals from the *Nepenthes* surface can be found on the tarsus of *C. morosus* (A). At higher magnification some pieces of wax can be seen on the arolium (B), but not on the hairs (C). Residues from the loose wax crystals adhere to the whole tarsus (D), cover the arolium (E) and make the tarsal hairs stick together (F).

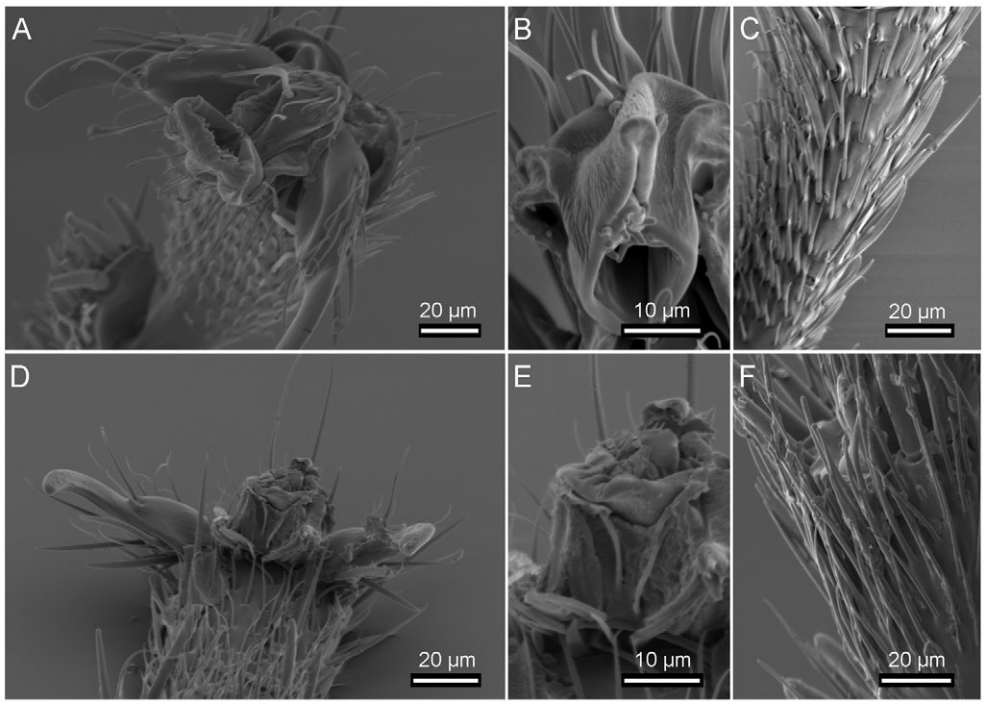

Fig. 8. Tarsi of the ant *Lasius niger* after slipping off the waxy surface of *N. alata* pitchers (A–C) and after walking on loose pieces of wax (D–F); SEM images. Slipping from the compact wax layer left only a slight residue on the tarsus (A), arolium (B) and hairs (C). Loose crystals of wax can be found in huge amounts on the whole tarsus (D) and especially on the arolium (E) and the tarsal hairs (F).

agglutinated to a certain degree and covering nearly the whole area of the last tarsal segments of *C. morosus*. The hairs on the tarsi are also covered with wax and are stuck together (Fig. 7F). Comparable results were found in *L. niger* (Fig. 8D–F); the hairs of all tarsal segments are stuck together by agglutinated waxes, and the claws and the arolia are also covered with wax crystals.

The second of these experiments was performed to test whether breakage of the waxy surface affects the arolii of the insects and consequently minimizes adhesion. The SEM images of *C. morosus* (Fig. 7A–C) and *L. niger* (Fig. 8A–C) after the experiments clearly show just a little wax residue on parts of the tarsi like the hairs and parts of the arolium. Even in higher magnification images only a small number of wax crystals and other indicators of wax residue from the waxy surface of the *Nepenthes* plant could be found on the arolium of *C. morosus* (Fig. 7B) and *L. niger* (Fig. 8B) or on the hairs and claws of the insects (Fig. 7C, Fig. 8C).

The third of the experiments was performed to test whether walking on loose wax crystals or on the intact wax layer of the conductive zone had any influence on the ants' ability to cling to smooth surfaces afterwards. The results are given as videos in the supplementary section (see supplementary material Movies 1–3). Those ants that walked on artificially detached wax clearly showed a reduced adhesion while walking on a vertical, smooth glass surface afterwards; thus, the friction force was below 1 $\boldsymbol{g}$ (where $\boldsymbol{g}$ is the gravitational acceleration). Contrary to those findings, ants walking on an intact pitcher surface showed no reduction of adhesion.

The above-mentioned findings indicate that detachment of individual platelets cannot be the main cause of the inability of insects to climb on the surface of the neck region of *N. alata*. In order to find out whether the structure itself or the mechanics are responsible for the described effect, we performed measurements of the adhesive forces of juvenile stick insects (*C. morosus*) on different artificial surfaces. In order to simulate the structure of the *N. alata* wax crystals, polishing paper of defined grain size was used. The silicon carbide crystals on polishing paper are platelet shaped and very thin and, thus, resemble the principal structural feature of the *N. alata* pitcher wax under investigation (Fig. 9). Because of their mechanical robustness, breakage of the silicon carbide crystals under the weight of a stick insect can be ruled out. For distinguishing between adhesion due to the adhesive pad (the arolium) and the claws of the insects, experiments were done with untreated animals and with insects where the claws had been removed. The frictional forces were measured using the centrifugation assay described above. The frictional force was defined as the centrifugal force at which detachment occurred. The results, normalized to the weight of the insects in units of the gravitational acceleration $\boldsymbol{g}$ are summarized in Fig. 10. Neat polycarbonate surfaces and polishing paper of different grain sizes (P4000–P320) were compared for untreated insects and insects with claws removed. It is evident that for untreated insects adhesion on the flat polycarbonate plates and on the rough polishing papers (P2000–P320) was fairly constant. However, the polishing paper P4000 was an exception as the insects could hardly adhere. They could not withstand a force that corresponds to an acceleration of 1 $\boldsymbol{g}$. Thus they were not able to walk or even stay on a vertical wall. The structure of P4000 shows a striking similarity of the grain dimensions with *N. alata* wax crystals (Fig. 9B). This finding was strongly supported by comparing the surface profile parameters of the two surfaces (Table 1). Both resemble thin and steep walls spaced by values (R_{Sm}) from 1.33 to 1.83 μm in the case of the polish paper and from 1.15 to 1.53 μm in the case of the *Nepenthes* surface. The R_a values of the polishing paper range from 0.241 to 0.448 μm and those of the *Nepenthes* surface from 0.17 to 0.369 μm. Insects with claws removed showed a different behaviour. While the adhesive force on the flat polycarbonate was similar to that observed for untreated insects, hardly any adhesion could be found on rough surfaces. Similar experiments performed with *L. niger* produced very similar results: while *L. niger* could withstand forces severalfold their own weight on the flat polycarbonate surface (acceleration of 26.6±14.5 $\boldsymbol{g}$) and on the polishing papers P320 (38.4±14.3 $\boldsymbol{g}$), P600 (23.9±7.3 $\boldsymbol{g}$) and P2000 (11.9±3.5 $\boldsymbol{g}$), they could hardly adhere on the P4000 surface (0.73±0.42 $\boldsymbol{g}$).

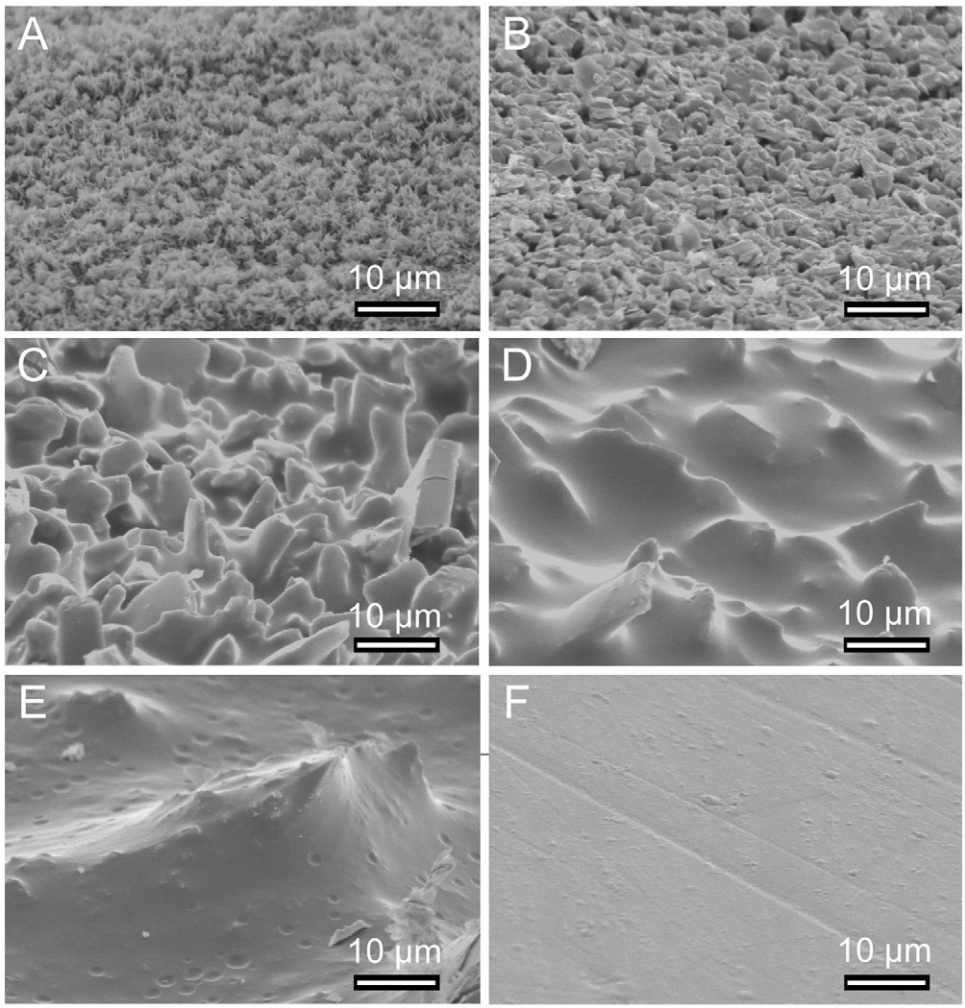

Fig. 9. SEM image of different test surfaces. (A) *Nepenthes alata*, (B–E) polishing papers P4000, P2000, P1000 and P320, respectively, and (F) polycarbonate. The surface of P4000 exhibits steep and thin walls of silicon carbide crystals. The size, shape and spacing of these crystals are very similar to the wax crystals of *N. alata* pitcher walls.

DISCUSSION

In the present study we could elucidate the 3D structure and investigate the mechanical properties of the epicuticular wax layer of the inner pitcher wall of *N. alata.* In the plant specimens in our hands we found the wax structures to be sponge-like (porous) with an outer pore size of about 1.3–1.5 µm, and to be mechanically very stable. There are some indications that the chemical composition and therefore probably the mechanical properties can change during maturation of the pitcher and according to environmental conditions (M.R. and M.R., unpublished data). However, until now we have failed to clarify under which conditions the wax layers become stable. Nevertheless, in the greenhouse-grown plant material we never found pitchers with crystals that broke under the weight of stick insects or ants or which could be broken by AFM scans. We cannot rule out the possibility that breaking of wax crystals may occur but what we clearly demonstrate is that the inner walls of the pitchers we investigated have stable crystals that are capable of catching prey. In this study we focused on insects having smooth pad-like adhesive organs. Ants were chosen as they are typical prey insects for *Nepenthes*. Additionally, stick insects were investigated because they are excellent model organisms which can be easily handled (much easier than ants) and for which mechanical parameters of the arolium are available (Scholz et al., 2008).

Stick insects were found to adhere well on artificial surfaces with either lower roughness like polycarbonate or higher roughness like polishing paper P2000 or lower. However, polishing paper with grain size P4000, which closely resembles the structure of *N. alata* wax crystals, allowed hardly any adhesion by the stick insects. When the claws of the stick insects were removed prior to the adhesion force measurements, the animals could adhere well on smoother surfaces like polycarbonate but failed to adhere to surfaces with greater roughness. This shows that the insect arolium is responsible for adhesion on flat surfaces whereas the claws perform well on rough surfaces. We propose that the surface of *N. alata* can exhibit a mechanically stable surface with a defined roughness which is too high for the arolium and too low for the claws to be effective.

For a formal approach we calculated the adhesion of a soft flat arolium and of a hard claw on a model surface, based on the profile parameters of P4000 and the *N. alata* wax crystals, as shown in

Table 1. Surface profile parameters of the glaucous conductive zone surface of *Nepenthes alata* pitchers and the polishing paper P4000

Surface profile parameter	*Nepenthes*	Polishing paper P4000
R_a (µm)	0.254±0.035	0.337±0.039
R_q (µm)	0.317±0.045	0.447±0.058
R_{Pc} (peaks per mm)	165 (±0.5 µm)	159 (±0.5 µm)
R_{Sm} (µm)	1.3±0.06	1.55±0.09

Comparing the parameters shows the similarity of the surfaces in terms of average roughness (R_a); root mean square roughness (R_q); roughness peak count (R_{Pc}); and the mean spacing of profile irregularities (R_{Sm}).

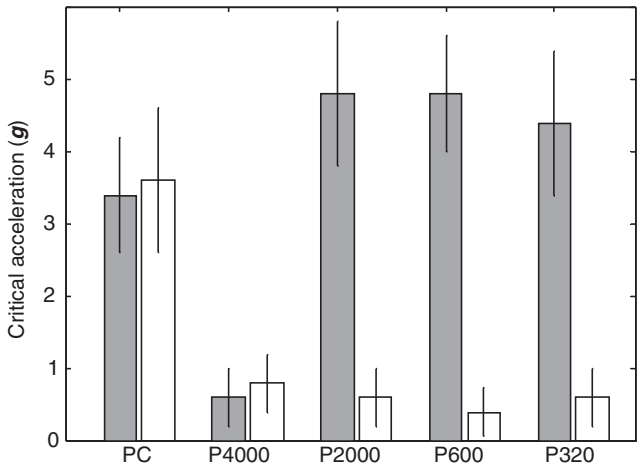

Fig. 10. The adhesion force of *C. morosus* on different artificial surfaces. Forces were measured by centrifugation of juvenile stick insects on either polycarbonate (PC), which is very flat, or polishing papers with varying grain size from P4000 (finest) to P320 (largest grain size). Untreated stick insects (filled bars) were able to adhere to the flat surface as well as to rough surfaces but hardly adhered to P4000, where they could not withstand forces corresponding to more than 1 ***g*** (acceleration >9.81 m s^{-2}). Insects with dissected claws (open bars) only adhered to the flat PC surface but not to the rough surfaces. Each bar represents the mean force ± s.d. of at least five individuals each measured three times.

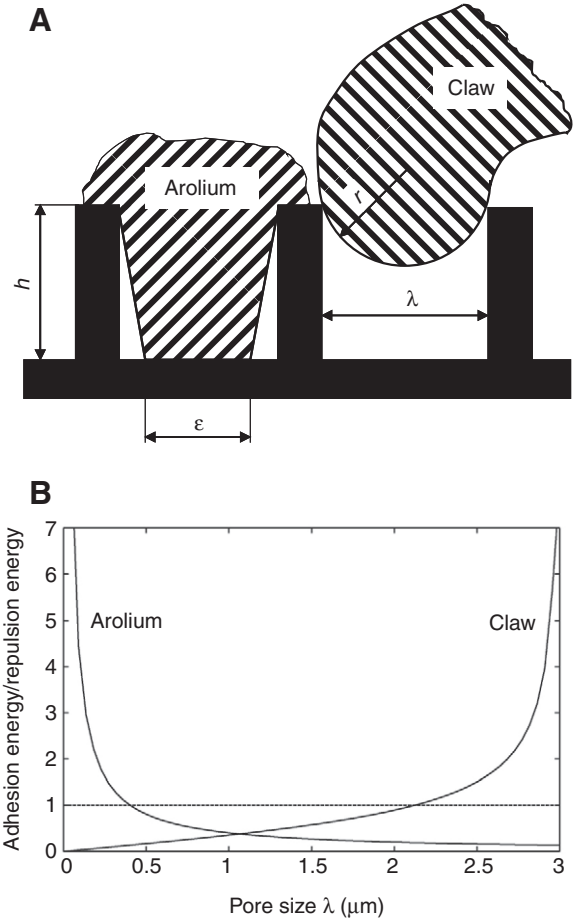

Fig. 11. Model of the *N. alata* pitcher wall surface and interactions with the arolium and/or a claw of an insect. (A) The surface is modelled for mathematical simplicity as a flat surface with walls of negligible thickness and height *h* which are spaced at a distance λ. For adhesion either a claw with tip radius *r* has to interact with the walls or the arolium has to deflect to form a frustum of a pyramid in order to have contact with the flat surface. The contact area is assumed to be a square of side length ε. (B) Plotting of the ratio of adhesive and repulsive energies due to arolium and claw according to the model described in the text reveals that the arolium adheres only to flat surfaces with a pore size (i.e. wall spacing) below about 0.5 μm where the ratio of adhesive and repulsive energy is above 1. In contrast, the claw allows adhesion only if the pore size is above about 2 μm. Thus, a small range of λ exists where neither the arolium nor the claw can achieve significant adhesion. The pore size λ of *N. alata* pitcher wall wax layers as well as that of the model surface P4000 is approximately 1–1.5 μm, which is exactly in the non-adhesive range.

Fig. 11A. For mathematical simplicity we assumed the surface to be a plane with upright walls of height h and negligible thickness. These walls are spaced at a distance λ, the pore size. For adhesion, either a claw with tip radius r has to interact with the walls or the arolium has to deflect to form a frustum of a pyramid in order to have contact with the flat surface. The contact area is assumed to be a square of side length ε. First we considered the adhesion due to the arolium. For this purpose we modified an approach for modelling of the adhesion of a very soft elastic body first described by Persson and colleagues (Persson et al., 2001) for the assumed geometry. Thus, in this case the adhesive energy is:

$$U_{\mathrm{A}} = -\Delta\gamma \times \varepsilon^2 , \qquad (1)$$

with Δγ comprising the free energy per surface area obtained when the flat surface interacts with the arolium. In order to allow adhesion, the absolute value of this energy has to be larger than the energy needed to form the contact, i.e. the repulsive energy. In our case this energy is the deformation energy U_{D} of the arolium, i.e. the energy necessary to mould the frustum out of the flat arolium. If $U_{\mathrm{A}}+U_{\mathrm{D}}<0$, adhesion occurs. Assuming the material of the arolium to be homogeneous and isomorphic, we can use the theory for deformation (indentation or buckling) of Oliver and Pharr (Oliver and Pharr, 2004). Given deformations in the linear elastic regime, the change of load (force) is given as:

$$\frac{\partial F_{\mathrm{D}}}{\partial h} = \frac{2\beta}{\sqrt{\pi}} \times E_{\mathrm{eff}} \times \sqrt{A} , \qquad (2)$$

with A being the cross-section of the indentation or buckling, β describing a material factor which is typically assumed to be 1, and E_{eff} standing for the effective elastic modulus of the arolium, which is defined as:

$$E_{\mathrm{eff}} = \frac{E}{1-\nu^2} , \qquad (3)$$

with E being Young's modulus and ν equalling Poisson's ratio.

Assuming the geometry depicted in Fig. 11A, the force necessary for deforming the flat surface in the described manner to form a frustum of height z is:

$$F_{\mathrm{D}} = \frac{2\beta}{\sqrt{\pi}} \times E_{\mathrm{eff}} \times \int_0^z \left(\varepsilon + \frac{(\lambda-\varepsilon)}{h} \times \varsigma \right) \mathrm{d}\varsigma . \qquad (4)$$

To obtain the deformation energy from Eqn 4, we have to integrate the force over the deformation z, which becomes:

$$U_{\mathrm{D}} = \int_0^h F_{\mathrm{D}}\, \mathrm{d}z = \frac{\beta \times E_{\mathrm{eff}} \times h^2}{3\sqrt{\pi}} \times (\lambda + 2\varepsilon) . \qquad (5)$$

For simplicity, we consider the negative ratio of the adhesive energy and the deformation energy. Adhesion occurs if $-U_A/U_D>1$. The ratio of the adhesive energy U_A and the deformation energy U_D follows as:

$$-\frac{U_A}{U_D}=\frac{3\times\Delta\gamma\times\varepsilon^2\times\sqrt{\pi}}{\beta\times E_{eff}\times h^2\times(\lambda+2\varepsilon)}\ . \quad (6)$$

The optimum for ε in the interval between 0 and λ is $\varepsilon=\lambda$. Setting the wall height $h=A\times\lambda$ with A being the constant ratio of pore size and wall height, Eqn 5 can be simplified to:

$$-\frac{U_A}{U_D}=\frac{\Delta\gamma\times\sqrt{\pi}}{A^2\times\beta\times E_{eff}\times\lambda}\ . \quad (7)$$

Thus the adhesiveness of the arolium on a surface scales with $1/\lambda$, i.e. the greater the roughness, the lower the adhesion. The contact energy per unit surface area $\Delta\gamma$ was estimated by Persson and colleagues (Persson et al., 2001) to be of the order of 40 mJ m^{-2}. The effective Young's modulus of the arolium of an adult *C. morosus* was recently determined by our group to be of the order of 10^5 N m^{-2} (Scholz et al., 2008). It is possible that the Young's modulus of the arolium cuticle will change with different larval states or over a period of time from lower to higher values, as is true for sclerotization of insect culticle. Considering this, the arolium of the juvenile stick insects might have lower Young's modulus values than the 10^5 N m^{-2}, and therefore be more flexible and provide a better adhesion than adult insects. Hence, our following calculation presents a kind of 'worst case scenario'. Assuming β and A are equal to 1, we obtain the dependency of the ratio of adhesive and repulsive energy due to the arolium according to Eqn 7 as depicted in Fig. 11B. In order to allow any adhesion, this ratio has to be larger than 1. The higher this ratio, the larger the additional force that can be transmitted by the adhesive contact.

The force which can be transmitted by the claws is dependent on the contact angle between the claw and the wall tip (Dai et al., 2002). This angle depends on the tip radius r of the claw tip and the pore size λ of the surface. In our SEM studies the tip radius of *C. morosus* was found to be about 7 μm and that of *L. niger* about 3 μm. If the pore size is larger than the diameter of the tip, the force, i.e. the adhesive energy, stays more or less constant. If $2r<\lambda$, the contact angle follows as $\arctan(\lambda/r)$. The ratio of the adhesive energy to the repulsive energy for the claw is given by the ratio of the contact angle and the friction angle, which is dependent on the materials in contact and which is equal to the arctan of the friction coefficient μ. Assuming a high friction angle of 30 deg., according to Dai and colleagues (Dai et al., 2002), we obtain the ratio of adhesive and repulsive energies for the claw as depicted in Fig. 11B. Obviously values above 1 require a pore size λ to be larger than about 2 μm. This behaviour is in line with recent observations (Dai et al., 2002).

Of course, the described theoretical model is only a first, rough estimation. However, it is based on experimentally obtained parameters and some conservative assumptions clearly showing that a small range of pore sizes (λ; the spacing between profile peaks in the case of polishing paper) exists, where neither the arolium nor the claws can adhere sufficiently to the surface. This range is between 0.5 and 2 μm, a result matching the pore sizes found for *N. alata* and the artificial surface P4000 having a pore size of approximately 1–1.5 μm.

The findings of this study show that the solid structure of the wax layer of the inner pitcher wall of *N. alata* together with the high hydrophobicity, which prevents wet adhesion, can explain the anti-adhesive properties of the conductive zone with respect to insect adhesive organs. Adhesion on the wax surface mediated by insect arolia can be excluded. The area of real contact between the arolium and the thin upwards-directed walls of the wax layer on the conductive pitcher surface is insufficient, because the thickness of the walls (clearly below 100 nm) and the given pore size of about 1 μm results in less than 10% effective contact area.

Thus, detachment of single wax crystals and contamination of the adhesive organs of insects is not necessary to explain the phenomena observed. Furthermore, the often-suggested detachment, which appears to play a major role for other plants [e.g. *Catopsis berteroniana* or *Brocchinia reducta* (Gaume et al., 2004); *Macaranga* spp. (I.S., M.B., L.D., T.E., A.W., F.H., J.M., S.H., M.R., M.R. and W.B., unpublished observations)] appears unlikely for the *Nepenthes* species investigated because of the mechanical properties of the wax layer measured experimentally. Indirect hints on the stability of *Nepenthes* wax crystals have already been given by Gaume and coworkers (Gaume et al., 2004). In their work they found contamination of the hairy adhesive organs of *C. vomitoria* after running for 10 min on intact plant surfaces of *C. berteroniana* and *B. reducta*, but only a small residue after running on *N. alata*. Massive contamination due to walking on *Nepenthes ventrata* surface could only be documented after 180 min, indicating the *N. ventrata* wax layer to be much more stabile. In a recent work, Gorb and coworkers (Gorb et al., 2005) found contamination of the hairy adhesive organs of *Adalia bipunctata* after 1 min of walking on *N. alata* surface which appears to be in contrast to the recent findings of Gaume and colleagues (Gaume et al., 2004) and the present study. This, once again, was found for hairy adhesive organs. For these organs breaking off material from the pitcher surface might be effective. However, it should be emphasized that the structure of the wax surface of *Nepenthes* is fully sufficient for catching prey with smooth adhesive organs like ants, which are the typical prey insects (Kato et al., 1993; Adam, 1997; Moran et al., 1999) under natural conditions. Furthermore, contamination of adhesive organs after minutes of walking on plant surfaces does not explain the immediate effect on insects trying to walk on the conductive zone of the pitcher, which results in instantaneous falling of the animal.

Lasius niger and *C. morosus* were chosen as experimental animals. The former were used because ants are the prey most frequently captured by *Nepenthes* plants, but they are not easy to handle in experiments. With *C. morosus* we used an insect which might not be a typical prey, but which has several advantages: first, the structure and the mechanical properties (elasticity module) of the adhesive organ are well documented; second, the insect has a much greater weight than the ants, which gives higher impact onto the wax layer of *Nepenthes*; third, stick insects are easy to handle.

Under these close-to-nature conditions the insects showed only a few wax crystals or residues on their tarsi, but nevertheless failed to adhere to the wax surface and slipped off. Comparing images of tarsi of *C. morosus* with those of *L. niger* after slipping showed only negligible contamination on the stick insect tarsi. This might be explained by the higher load per area of the animals. Based on measurements of the contact area of adult specimens of *C. morosus* (Drechsel and Federle, 2006) and ants of the genus *Oecophylla smaragdina* (Endlein and Federle, 2008), the load of a juvenile stick insect is about 20–30 times higher (about 9–12 mN mm^{-2} in comparison to about 0.42 mN mm^{-2} load for *L. niger*). Additionally, in the third part of our slip-off experiments we clearly showed that only artificially detached wax from the conductive zone of the pitcher leads to a reduced adhesion of insects on a smooth surface. Walking on the intact wax layer had no such effect.

These findings strongly support the theory of a stable wax-foam surface that minimizes adhesion by its surface parameters even if bigger insects try to adhere.

In conclusion we cannot rule out the possibility that to a certain degree breaking of extensively protruding single wax crystals may occur and consequently be found as residues attached to the tarsi. Presumably this would increase the anti-adhesive effect of the surface of *N. alata*. Furthermore, breaking of crystals for catching prey may occur in different species of pitcher plants or even individuals of *N. alata* under certain circumstances or environmental conditions. However, the results presented clearly indicate that the structural properties of the mechanically very stabile epicuticular wax alone are sufficient to prevent insect adhesion to the conductive zone of *N. alata*.

ACKNOWLEDGEMENTS

The authors thank Dr Walter Federle (Cambridge, UK) for helpful discussion and comments on the manuscript. The work was financially supported by grants from the Deutsche Forschungsgemeinschaft (SFB 567 'Mechanisms of interspecific interactions of organisms' and SPP 1207 'Strömungsbeeinflussung in der Natur und Technik'). We are also indebted to the staff of the Botanical Garden of the University of Würzburg for cultivating the plants used. Deposited in PMC for immediate release.

REFERENCES

Adam, J. H. (1997). Prey spectra of Bornean *Nepenthes* species (Nepenthaceae) in relation to their habitat. *Pertanika J. Trop. Agric. Sci.* **20**, 121-134.

An, C. I., Fukusaki, E. and Kobayashi, A. (2002a). Aspartic proteinases are expressed in pitchers of the carnivorous plant *Nepenthes alata* Blanco. *Planta* **214**, 661-667.

An, C. I., Takekawa, S., Okazawa, A., Fukusaki, E. and Kobayashi, A. (2002b). Degradation of a peptide in pitcher fluid of the carnivorous plant *Nepenthes alata* Blanco. *Planta* **215**, 472-477.

Bauer, U., Bohn, H. F. and Federle, W. (2008). Harmless nectar source or deadly trap: Nepenthes pitchers are activated by rain, condensation and nectar. *Proc. Biol. Sci.* **275**, 259-265.

Beutel, R. G. and Gorb, S. N. (2001). Ultrastructure of attachment specializations of hexapods (Arthropoda): evolutionary patterns inferred from a revised ordinal phylogeny. *J. Zool. Syst. Evol. Res.* **39**, 177-207.

Bohn, H. F. and Federle, W. (2004). Insect aquaplaning: *Nepenthes* pitcher plants capture prey with the peristome, a fully wettable water-lubricated anisotropic surface. *Proc. Natl. Acad. Sci. USA* **101**, 14138-14143.

Dai, Z., Gorb, S. N. and Schwarz, U. (2002). Roughness-dependent friction force of the tarsal claw system in the beetle *Pachnoda marginata* (Coleoptera, Scarabaeidae). *J. Exp. Biol.* **205**, 2479-2488.

Drechsler, P. and Federle, W. (2006). Biomechanics of smooth adhesive pads in insects: influence of tarsal secretion on attachment performance. *J. Comp. Physiol. A* **192**, 1213-1222.

Endlein, T. and Federle, W. (2008). Walking on smooth or rough ground: passive control of pretarsal attachment in ants. *J. Comp. Physiol. A* **194**, 49-60.

Federle, W., Rohrseitz, K. and Hölldobler, B. (2000). Attachment forces of ants measured with a centrifuge: better 'wax-runners' have a poorer attachment to smooth surface. *J. Exp. Biol.* **203**, 505-512.

Federle, W., Baumgartner, W. and Hölldobler, B. (2004). Biomechanics of ant adhesive pads: frictional forces are rate- and temperature-dependent. *J. Exp. Biol.* **207**, 67-74.

Gaume, L. and Forterre, Y. (2007). A viscoelastic deadly fluid in carnivorous pitcher plants. *PLoS ONE* **2**, e1185.

Gaume, L., Gorb, S. and Rowe, N. (2002). Function of epidermal surfaces in the trapping efficiency of *Nepenthes alata* pitchers. *New Phytol.* **156**, 479-489.

Gaume, L., Perret, P., Gorb, E., Gorb, S., Labat, J. J. and Rowe, N. (2004). How do plant waxes cause flies to slide? Experimental tests of wax-based trapping mechanisms in three pitfall carnivorous plants. *Arthropod. Struct. Dev.* **33**, 103-111.

Gorb, E., Haas, K., Henrich, A., Enders, S., Barbakadze, N. and Gorb, S. N. (2005). Composite structure of the crystalline epicuticular wax layer of the slippery zone in the pitchers of the carnivorous plant *Nepenthes alata* and its effect on insect attachment. *J. Exp. Biol.* **208**, 4651-4662.

Juniper, B. E. and Burras, J. K. (1962). How pitcher plants trap insects. *New Sci.* **269**, 75-77.

Juniper, B. E., Robins, R. J. and Joel, D. M. (1989). *The Carnivorous Plants*. London: Academic Press.

Kato, M., Hotta, M., Tamin, R. and Itino, T. (1993). Inter- and intra-specific variation in prey assemblages and inhabitant communities in *Nepenthes* pitchers in Sumatra. *Trop. Zool.* **6**, 11-25.

Knoll, F. (1914). Über die Ursache des Ausgleitens der Insektenbeine an wachsbereiften Pflanzenteilen. *Jahrbücher Wissenschaftlicher Botanik* **54**, 448-497.

Lloyd, F. E. (1942). *The Carnivorous Plants*. New York: Ronald Press.

McFarlane, J. M. (1893). Observations on pitchered insectivorous plants, part. II. *Ann. Bot.* **7**, 401-458.

Moran, J. A. (1996). Pitcher dimorphism, prey composition and the mechanisms of prey attraction in the pitcher plant *Nepenthes rafflesiana* in Borneo. *J. Ecol.* **84**, 515-525.

Moran, J. A., Booth, W. E. and Charles, J. K. (1999). Aspects of pitcher morphology and spectral characteristics of six Bornean *Nepenthes* pitcher plant species: implications for prey capture. *Ann. Bot.* **83**, 521-528.

Oliver, W. C. and Pharr, G. M. (2004). Measurement of hardness and elastic modulus by instrumented indentation: Advances in understanding and refinements to methodology. *J. Mater. Res.* **19**, 3-20.

Owen, T. P. and Lennon, K. A. (1999). Structure and Development of the pitchers from the carnivorous plant *Nepenthes alata* (Nepenthaceae). *Am. J. Bot.* **86**, 1382-1390.

Owen, T. P., Lennon, K. A., Santo, M. J. and Anderson, A. N. (1999). Pathways for nutrient transport in the pitchers of the carnivorous plant *Nepenthes alata*. *Ann. Bot.* **84**, 459-466.

Persson, B. N. J. and Tosatti, E. (2001). The effect of surface roughness on the adhesion of elastic solids. *J. Chem. Phys.* **115**, 5597-5610.

Riedel, M., Eichner, A. and Jetter, R. (2003). Slippery surfaces of carnivorous plants: composition of epicuticular wax crystals in *Nepenthes alata* Blanco pitchers. *Planta* **218**, 87-97.

Riedel, M., Eichner, A., Meimberg, H. and Jetter, R. (2007). Chemical composition of epicuticular wax crystals on the slippery zone in pitchers of five *Nepenthes* species and hybrids. *Planta* **225**, 1517-1534.

Scholz, I., Baumgarnter, W. and Federle, W. (2008). Micromechanics of smooth adhesive organs in stick insects: pads are mechanically anisotropic and softer towards the adhesive surface. *J. Comp. Physiol. A* **194**, 373-384.

Schulze, W., Schulze, E. D., Pate, J. S. and Gillison, A. N. (1997). The nitrogen supply from soils and insects during growth of the pitcher plants *Nepenthes mirabilis*, *Cephalotus follicularis* and *Darlingtonia californica*. *Oecologia* **112**, 464-471.